Atmos. Chem. Phys. Discuss., 10, 7383–7419, 2010
www.atmos-chem-phys-discuss.net/10/7383/2010/

Atmospheric Chemistry and Physics Discussions

This discussion paper is/has been under review for the journal Atmospheric Chemistry and Physics (ACP). Please refer to the corresponding final paper in ACP if available.

Measurement of atmospheric nitrous acid at Blodgett Forest during BEARPEX2007

X. Ren[1], H. Gao[2], X. Zhou[2,3], J. D. Crounse[4], P. O. Wennberg[5,6], E. C. Browne[7], B. W. LaFranchi[7,*], R. C. Cohen[7,8], M. McKay[**], A. H. Goldstein[9], and J. Mao[10,*]**

[1]Rosenstiel School of Marine and Atmospheric Science, University of Miami, Miami, FL, USA
[2]Department of Environmental Health Sciences, State University of New York at Albany, Albany, NY, USA
[3]Wadsworth Center, New York State Department of Health, Albany, NY, USA
[4]Division of Chemistry and Chemical Engineering, California Institute of Technology, Pasadena, CA, USA
[5]Division of Engineering and Applied Sciences, California Institute of Technology, Pasadena, CA, USA
[6]Division of Geological and Planetary Sciences, California Institute of Technology, Pasadena, CA, USA
[7]Department of Chemistry, University of California at Berkeley, Berkeley, CA, USA
[8]Department of Earth and Planetary Science, University of California at Berkeley, Berkeley, CA, USA

[9]Department of Environmental Science, Policy, and Management, University of California at Berkeley, Berkeley, CA, USA
[10]Department of Meteorology, Pennsylvania State University, University Park, PA, USA
[*]now at: Center for Accelerator Mass Spectrometry, Lawrence Livermore National Laboratory, Livermore, CA, USA
[**]now at: California Air Resources Board, Sacramento, CA, USA
[***]now at: School of Engineering and Applied Sciences, Harvard University, Cambridge, MA, USA

Received: 11 March 2010 – Accepted: 17 March 2010 – Published: 22 March 2010

Correspondence to: X. Ren (xren@rsmas.miami.edu)

Published by Copernicus Publications on behalf of the European Geosciences Union.

Abstract

Nitrous acid (HONO) is an important precursor of the hydroxyl radical (OH) in the lower troposphere. Understanding HONO chemistry, particularly its sources and contribution to HO_x (=OH+HO_2) production, is very important for understanding atmospheric oxidation processes. A highly sensitive instrument for detecting atmospheric HONO based on aqueous long path absorption photometry (LOPAP) was deployed in the Biosphere Effects on Aerosols and Photochemistry Experiment (BEARPEX) at Blodgett Forest, California in late summer 2007. The median diurnal variation shows minimum HONO levels of about 20–30 pptv during the day and maximum levels of about 60–70 pptv at night, a diurnal pattern quite different from the results at various other forested sites. Measured HONO/NO_2 ratios for a 24-h period ranged from 0.05 to 0.13 with a mean ratio of 0.07. Speciation of reactive nitrogen compounds (NO_y) indicates that HONO accounted for only ~3% of total NO_y. However, due to the fast HONO loss through photolysis, a strong HONO source (1.59 ppbv day^{-1}) existed in this environment in order to sustain the observed HONO levels, indicating the significant role of HONO in NO_y cycling. The LOPAP HONO measurements were compared to the HONO measurements made with a Chemical Ionization Mass Spectrometer (CIMS) over a three-day period. Good agreement was obtained between the measurements from the two different techniques. Using the expansive suite of photochemical and meteorological measurements, the contribution of HONO photolysis to HO_x budget was calculated to be relatively small (6%) compared to results from other forested sites. The lower HONO mixing ratio and thus its smaller contribution to HO_x production are attributed to the unique meteorological conditions and low acid precipitation at Blodgett Forest. Further studies of HONO in this kind of environment are needed to test this hypothesis and to improve our understanding of atmospheric oxidation and nitrogen budget.

1 Introduction

Nitrous acid (HONO) plays an important role in atmospheric chemistry because its photolysis results in the formation of the hydroxyl (OH) radical, the key atmospheric oxidant that initiates the oxidation of many primary and secondary pollutants leading to the formation of ozone and fine particles. Previous studies have found HONO photolysis to be a major or an important OH source in forested (Winer and Biermann, 1994; Harrison et al., 1996; Alicke et al., 2003; Kleffmann et al., 2005; Ren et al., 2006) and urban environments (Alicke et al., 2003; Ren et al., 2003; Acker et al., 2006a; Mao et al., 2010). Measurement of HONO within these environments can reveal the contribution of HONO photolysis to HO_x (=$OH+HO_2$) radical production and oxidation capacity. Furthermore, recent studies have demonstrated that the photolysis of HONO is an important OH source, not only in the early morning when other OH sources (such as the photolysis of O_3) are still small, but also throughout the day. This indicates the existence of a strong daytime OH source from HONO photolysis. In these studies, the contribution of HONO photolysis to HO_x production was often found to be greater than or comparable to the contribution from the photolysis of ozone and formaldehyde (Neftel et al., 1996; Staffelbach et al., 1997; Zhou et al., 2002a; Kleffmann et al., 2002, 2003, 2005, 2006; Vogel et al., 2003; Acker et al., 2006b, 2007; Ren et al., 2003, 2006; Elshorbany et al., 2009; Mao et al., 2010).

Despite the importance of HONO in atmospheric chemistry, HONO source strengths and its detailed formation mechanisms, especially during daytime, are not well understood. In addition to the homogeneous HONO formation from the reaction of NO with OH, Li et al. (2008) found that the reaction of photolytically excited NO_2 with water can form HONO and OH, but its reaction rate and yield are still under debate (Carr et al., 2009) and this mechanism likely contributes insignificantly to atmospheric HONO formation. Models taking into account only the homogeneous HONO sources typically predict significantly lower HONO concentrations than measurements. Heterogeneous processes are thus considered as major HONO sources, along with the homogeneous

ACPD
10, 7383–7419, 2010

formation and direct emissions from combustion processes. Major heterogeneous processes to form HONO include: (1) heterogeneous conversion of NO_2 adsorbed on humid surfaces (Finlayson-Pitts et al., 2003; Langridge et al., 2009); (2) photosensitized reduction of NO_2 on organic surfaces such as aromatics and humic acids (George et al., 2005; Stemmler et al., 2006; Qin et al., 2009), and (3) photolysis of surface adsorbed nitric acid (HNO_3) and nitrate (Zhou et al., 2001; 2002b; 2003). Heterogeneous conversion of NO_2 on fresh soot particles and secondary organic aerosols can also form HONO (Ammann et al., 1998; Arens et al., 2001; Bröske et al., 2003; Ziemba et al., 2010), but the roles of these processes are still under discussion (Arens et al., 2001; Bröske et al., 2003; Aubin et al., 2007; Qin et al., 2009). Lastly, photolysis of o-nitrophenol and its methylated analogues can produce HONO (Bejan et al., 2006), but this mechanism is only important in urban areas where concentrations of nitrophenols are high.

Comparison of different techniques for detecting HONO is vital to evaluate and enhance their capabilities. This type of intercomparison has been conducted in field campaigns, especially between well accepted long path differential optical absorption spectroscopy (LP-DOAS) and chemical techniques such as denuder (Appel et al., 1990; Febo et al., 1996; Spindler et al., 2003), long path absorption photometry (LOPAP) (Heland et al., 2001; Kleffmann et al., 2006; Acker et al., 2006a), and mist chamber (Stutz et al., 2010). The results in these studies showed consistent agreement in general, although occasionally there were significant differences that could be explained by either an NO_2 artifact of the DOAS instruments or possible interferences in the chemical methods (Heland et al., 2001; Kleffmann et al., 2006; Stutz et al., 2010). Excellent agreement has been obtained between LOPAP and LP-DOAS (Acker et al., 2006a; Kleffmann et al., 2006). Chemical Ionization Mass Spectrometry (CIMS) has proven to be a powerful technique to measure many atmospheric trace gases. It has been used to measure HONO in the laboratory (Hirokawa et al., 2009), but rarely in the real atmosphere (Yokelson et al., 2009). Comparison of this new technique with other established techniques for HONO measurement is of particular interest.

Here we present HONO measurement results from the Biosphere Effects on Aerosols and Photochemistry Experiment (BEARPEX) at Blodgett Forest, California in late summer 2007. The mixing ratios and diurnal profile of atmospheric HONO at this site are compared to results obtained from other forested sites. HONO measurements made by LOPAP and CIMS are compared over three days. Using other concurrent measurements of trace gases and meteorological parameters, a box model was developed and the contribution of HONO photolysis to HO_x production was calculated.

2 Experimental

2.1 Site description

Measurements of HONO were made within a ponderosa pine plantation adjacent to the University of California at Berkeley's Blodgett Forest Research Station (BFRS). The site is located in the western foothills of the Sierra Nevada mountains (38°58′42.4″ N, 120°38′3.4″ W, 1315 m elevation), ~75 km northeast of Sacramento, CA. Average tree height within the daytime fetch was 7.9 m, and leaf area index (LAI) was estimated as 3.2 $m^2 m^{-2}$ (Wolfe et al., 2009). Typical meteorological conditions at the site have been described in detail elsewhere (e.g., Goldstein et al., 2000; LaFranchi et al., 2009; Wolfe et al., 2009; Bouvier-Brown et al., 2009). Briefly, the meteorology during the dry season (May–September) is characterized by high daytime temperatures, low rainfall, low humidity, clear skies, and consistent southwesterly (upslope) wind during the day and northeasterly (downslope) wind at night. During the wet season (October–April), winds are less regular, temperatures are cooler, and there is moderate rainfall and snowfall.

The site contained two sampling towers: an original 15 m walk-up tower, and a new 18 m scaffolding tower located ~20 m north of the old tower. Inlets for HONO instruments were located on the north tower. Other measurements used in our analyses were taken on, or directly adjacent to, the north tower. Power was provided by a propane generator situated 125 m north of the new tower, perpendicular to our sampling location and the prevailing daytime wind direction. As in previous studies at this site, occasional short-duration plumes from the generator were often detected only during nighttime when winds were weak and variable in direction. HONO measurements with the influence of the generator plumes have been excluded from the analysis.

2.2 Description of measurement techniques

2.2.1 Long Path Absorption Photometer (LOPAP)

The first technique for measurement of atmospheric HONO is based on aqueous scrubbing followed by nitrite derivatization to a highly light-absorbing azo dye, which is then detected with a long path absorption photometer (LOPAP) (Heland et al., 2001; Kleffmann et al., 2002; Huang et al., 2002; Zhou et al., 2002a). The derivatization to the azo dye is completed through the following nitrite reactions with sulfanilamide (SA) and N-(1-naphthyl) ethylenediamine (NED):

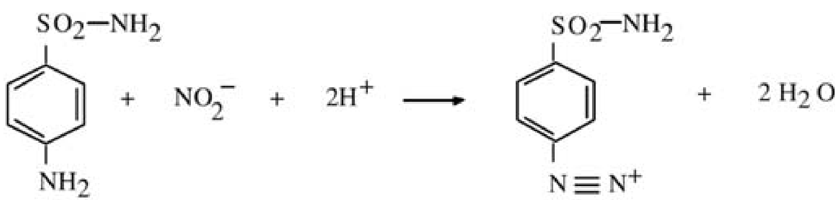

(SA) (Diazonium) (R1)

ACPD
10, 7383–7419, 2010

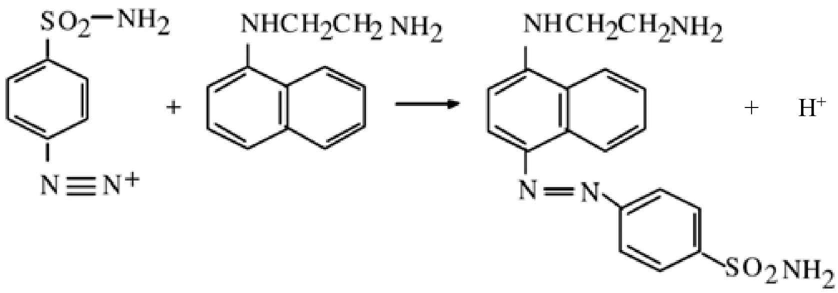

(NED) (Azo dye) (R2)

A custom-built LOPAP instrument was deployed in this study. Ambient air was pulled through 10-turn glass coil samplers by a vacuum pump and the air flow rates were controlled by mass flow controllers. A phosphate buffer with a concentration of $1.0\,\mathrm{mmol\,L^{-1}}$ was used as a scrubbing solution to collect HONO in the air sample. Due to its large effective Henry's Law constant (Park and Lee, 1988), HONO in the air was quantitatively collected in the samplers, confirmed in the collection efficiency experiment (see Sect. 2.3.2). After the separation from the gas phase, the scrubbing solution was mixed with SA/NED reagents. The mixture was then pumped through a Teflon derivatization tubing, where nitrite was converted to the azo dye via the above two Reactions (R1) and (R2). The aqueous sample finally flowed through a liquid waveguide capillary cell (LWCC, World Precision Instruments). The absorption of the light from a tungsten light source (FO-6000, World Precision Instruments) by azo dye in the sample was measured using a USB spectrometer (USB4000, Ocean Optics). The scrubbing solution and reagent solutions were delivered using a 16-channel peristaltic pump (Ismatec).

The LOPAP instrument was calibrated using sodium nitrite ($NaNO_2$) standard solutions as well as a HONO generation system as described below. The HONO mixing ratios in air samples can be calculated using the following equation:

$$[\mathrm{HONO}]_{\mathrm{pptv}} = \frac{C_l F_l \mathrm{RT}}{F_g P} \times 10^{12} \tag{1}$$

where, C_l is nitrite concentration ($\mathrm{mol\,L^{-1}}$) in the scrubbing solution, F_l is the flow rate ($\mathrm{cm^3\,min^{-1}}$) of the scrubbing solution, F_g is the sampling air flow rate ($\mathrm{L\,min^{-1}}$), R is the gas constant ($8.314\,\mathrm{Pa\,m^3\,K^{-1}\,mol^{-1}}$), and T and P are the temperature (294 K) and atmospheric pressure (101 325 Pa) under which the mass flow controllers were calibrated. The detection limit of the LOPAP instrument was about 3 pptv with a 2-min integration time and the measurement uncertainty was about ±15% at a 2σ confidence level.

2.2.2 Chemical Ionization Mass Spectrometer (CIMS)

During this study, HONO was also monitored by the Caltech chemical ionization mass spectrometer (Caltech-CIMS) using the CF_3O^- reagent ion, via the fluoride transfer product ion channel (m/z=66, $HFNO_2^-$).

$$CF_3O^- + HONO \rightarrow HFNO_2^- + CF_2O \tag{R3}$$

The instrument was situated on top of the north tower during this study with an inlet height of ∼17.7 m above ground level. Due to the time needed to measure other chemical species, the ion channel m/z=66 was only monitored 2.8% of the time (i.e., 0.5 s every 18 s). Instrument zeros were conducted approximately once every 15 min by passing ambient air through a filter filled with nylon wool that was coated with sodium bicarbonate. In-situ calibrations were conducted approximately once every 1.5 h using H_2O_2 and HNO_3 standards, and proxied to HONO using laboratory calibrations curves. The primary interference to the HONO signal, formic acid product ion ($^{13}CH(O)O^-HF$), has been removed using the signal at m/z=65 ($^{12}CH(O)O^-HF$). Additional detailed

ACPD
10, 7383–7419, 2010

information about this instrument can be found elsewhere (Crounse et al., 2006). The precision for a 0.5-s integration period was about 25 pptv (1σ).

The Caltech-CIMS was operational between 15 August and 27 September 2007 with the exception of several periods of downtime due to rain and technical difficulties. The LOPAP HONO measurements covered the period between 25 September and 10 October 2007. Both LOPAP and CIMS measured HONO on three overlapping days, 25–27 September, allowing for the HONO intercomparison between LOPAP and CIMS.

2.2.3 Other measurements

Other concurrent measurements used in this analysis include ozone based on UV absorption, NO_2, alkyl nitrates (ANs) and peroxy nitrates (PNs) based on thermo-dissociation laser induced fluorescence (TD-LIF) (Thornton et al., 2000), OH and HO_2 based on laser-induced fluorescence (Faloona et al., 2004), and meteorological parameters, including ambient temperature, pressure, relative humidity, wind direction, wind speed, and solar radiation. There were no direct measurements of photolysis frequencies (J values). The NCAR Tropospheric Ultraviolet and Visible (TUV) transfer model (http://www.acd.ucar.edu/TUV) was used to calculate clear sky J values with the O_3 column density measured by the Total Ozone Mapping Spectrometer (TOMS, data available at http://toms.gsfc.nasa.gov/teacher/ozone_overhead.html). In order to correct for solar attenuation by clouds, the calculated J values on a clear day were used to calculate a cloudiness factor. The field experiment log and the profile of the solar radiation measured on 1 September 2007 indicated that it was a clean day with a clear sky. Thus the ratio of clear-sky photolysis frequency to solar radiation intensity for each photolytic species on this day was calculated and used as a reference to correct the cloud attenuation. The J values on other days were then scaled to the measured solar radiation intensity.

During this study, the measurement of NO failed due to technical difficulties. Previous studies at this site have found that NO, NO_2, and O_3 approximately reached photostationary state (PSS) during midday (e.g., Day et al., 2009). With the PSS approximation

ACPD
10, 7383–7419, 2010

and the concurrent measurements of NO_2, O_3 and HO_2, daytime NO concentrations were calculated using Eq. (2):

$$[NO]_{SS} = \frac{J_{NO_2}[NO_2]}{k_{O_3+NO}[O_3] + k_{HO_2+NO}[HO_2] + \sum_i k_{RO_{2i}+NO}[RO_{2i}]} \quad (2)$$

Peroxy radicals were not measured and we assume that total RO_2 levels were 1.6 times HO_2 levels, a median daytime RO_2/HO_2 ratio in the box model. We also assume that the rate coefficients for the RO_2+NO reactions are the same as the rate coefficient for the CH_3O_2+NO reaction. Nighttime NO concentrations are assumed to be the same as the mean nighttime concentrations measured during BEARPEX2009 in summer 2009. As NO only contributed a small fraction (2–10%) to NO_y at this site (Fig. 8), the uncertainty in the calculated NO does not significantly affect the NO_y speciation (Sect. 3.4).

2.3 Laboratory characterization of the LOPAP instrument

2.3.1 HONO generation system

A HONO generation system was developed to quantitatively produce HONO with high purity and high stability. It is based on the reaction between gaseous hydrogen chloride (HCl) and solid sodium nitrite ($NaNO_2$) (Febo et al., 1995):

$$NaNO_{2(s)} + HCl_{(g)} \rightarrow HONO_{(g)} + NaCl_{(s)} \quad (R4)$$

The gaseous HCl was produced using a piece of thin-wall Teflon tubing that was immersed into a concentrated hydrochloric acid solution (9–12 mol L^{-1}, Fig. 1). A small zero air flow was introduced into the Teflon tubing as a carrier gas. Because of the partial pressure difference in $HCl_{(g)}$ between the inside and outside of the Teflon tubing, small amount of gas phase HCl diffused into the carrier gas. The produced HCl/air mixture was mixed with some humidified air produced with a water bubbler before entering a small reactor containing $NaNO_2$ powder (the $NaNO_2$-HCl reactor), where the $NaNO_2$+HCl reaction occurred. The produced HONO flow was diluted by zero air before it was measured by an NO-NO_x analyzer (TEI, Model 42i-TL, Thermo Fisher) and/or the LOPAP instrument. The NO-NO_x analyzer contains a molybdenum catalytic converter to quantitatively convert HONO into NO followed by the chemiluminescence detection of NO. These chemiluminescence detectors with molybdenum converters have been proven to have near unit response to HONO (Allegrini et al., 1990; Pérez et al., 2007). In order to stabilize the HONO levels from the calibration source, the temperature of the hydrochloric acid solution and the $NaNO_2$-HCl reactor, as well as the humidity in the air through the $NaNO_2$-HCl reactor were controlled. The produced HONO levels can be varied over three orders, from a few tens of pptv to a few tens of ppbv by varying the length of the Teflon tubing immersed into the hydrochloric acid, the concentration and temperature of hydrochloric acid, and the dilution flow rate of zero air.

The HONO generation system was tested in the laboratory and the produced HONO was sampled simultaneously by the LOPAP instrument and the NO-NO_x analyzer. The LOPAP instrument was calibrated using standard solutions of $NaNO_2$ and the NO-NOx analyzer was calibrated with a cylindered NO calibration mixture (9.96 ppmv of NO in N_2 with a ±2% uncertainty, Matheson Tri-Gas). Very good agreement was obtained between the two measurements (Fig. 2), suggesting the reliability of the LOPAP instrument and HONO generation system.

2.3.2 Collection efficiency and delay time

In addition to the calibration of the LOPAP instrument, the HONO generation system was used to characterize the collection efficiency and delay time (the time when an air sample reaches the samplers to the time when the sample signal appears in the detection cell) of the LOPAP instrument. The coil samplers used in this study have an uptake efficiency of (99.6±0.5)% for HONO at a sampling flow rate of 2 L min^{-1}. The

ACPD
10, 7383–7419, 2010

instrument delay time was 12.9±0.8 min, which includes the derivatization time (5 min) and the time for the reagent solutions to flow through autoanalysis tubings attached onto the peristaltic pump.

2.4 Interference tests

HONO measurements based on chemical methods can suffer from a variety of interferences (Kleffmann and Wiesen, 2008; Stutz et al., 2010). Therefore HONO instruments based on wet chemistry need to be carefully designed and characterized. Heland et al. (2001) and Huang et al. (2002) have tested several possible interferences for their instruments and all tested species showed insignificant interferences to HONO measurement. In the laboratory, we also tested several candidate chemicals, including NO_2, HNO_3, nitrate, and SO_2, for possible interferences in our HONO instrument.

NO_2 is slightly soluble in liquid water with a Henry's Law constant of $0.01\,mol\,L^{-1}\,atm^{-1}$ (Schwartz and White, 1981). Assuming that the air sample contains 100 ppbv of NO_2 at 1 atm pressure and NO_2 reaches equilibrium when air passes through the glass coil sampler, the concentration of the formed nitrous acid in the aqueous phase is about $1.0\,nmol\,L^{-1}$, which corresponds to 3.4 pptv of HONO under typical sample conditions. Zero air containing approximately 100 ppbv of NO_2 was used to test the actual NO_2 interference to the HONO measurement. The NO_2 – air mixture was generated by an NO_2 permeation tube (VICI Metronics) using a Dynacalibrator (VICI Metronics). There was an observed small fraction of HONO (about 1% of NO_2 level) in the NO_2 source, either existing in the NO_2 permeation tube or formed on the surfaces inside the Dynacalibrator. In order to test the true interference from NO_2, the NO_2 mixture was passed through a dry glass annular denuder (URG) coated with sodium carbonate. The denuder removed all HONO but only removes about 5% of NO_2. The interference was found to be about 20 pptv of HONO per 100 ppbv of NO_2, or 0.02% of NO_2, which is small considering the relatively low NO_2 levels at Blodgett Forest (i.e., up to ~3 ppbv of NO_2, which corresponds to an interference level of ~0.6 pptv of HONO). This interference level is comparable to what was found by Heland et al. (2001) with

ACPD
10, 7383–7419, 2010

an interference level of (0.011±0.005)%, but greater than the estimation based on the Henry's Law constant of NO_2, possibly due to the NO_2 reaction with H_2O, leading to a larger effective NO_2 solubility than the equilibrium based on the Henry's Law.

Possible interferences from HNO_3 and nitrate were tested using an HNO_3 permeation tube (VICI Metronics) to generate an air flow with an HNO_3 mixing ratio of ∼5 ppbv or using sodium nitrate standard solutions (80–400 nmol L^{-1}). There was no detectable interference (below the detection limit) in either test. Interference from SO_2 was tested with an SO_2/air mixture containing an SO_2 mixing ratio of ∼50 ppbv, which was sampled by the LOPAP instrument. The interference was also found to be small and negligible.

In the field, another interference test was conducted using a dry annular denuder coated with sodium carbonate by connecting the denuder to the sampling inlet. The test was designed to characterize interferences from aerosols and other nitrogen species (e.g., NO_x, PAN, and other organic nitrates) in air samples by removing HONO but retaining most of particles, NO_2, PAN or other organic nitrates in the air flow. The signals obtained from the ambient air through the denuder were essentially the same as the signals from zero air, indicating that there were no significant HONO interferences from the possible interfering species such as NO_2, aerosols, and organic nitrates in this environment.

3 Results and discussion

3.1 Measurements of meteorological parameters and trace gases

Shown in Fig. 3 are meteorological measurements from the last two weeks of the BEARPEX2007 study, when the LOPAP HONO measurements were available. Summer 2007 was cooler than usual. There were slight rainfalls on nights of 28/29 September and 9/10 October. An early snowfall came on 5 October 2007. During this period, wind directions were less regular due to a few cold fronts crossing over the site (Fig. 3).

HONO measurements made by the LOPAP during the last two weeks of BEARPEX2007 exhibit a large variability ranging from near 0 to 160 pptv (Fig. 4). Meteorological conditions affected the HONO mixing ratio significantly at this forested site. For example, a rapid drop in HONO mixing ratios from near 100 pptv to ∼25 pptv at ∼21:30 (PST) on 28 September (Fig. 4) was primarily caused by a rapid wind shift from southwesterly to northerly followed by a slight rainfall. Another example of meteorological influence on HONO took place on the night of 9/10 October when the wind started to shift from southwesterly to easterly at ∼17:00 (PST). In about two hours, the wind shifted back to southerly and remained in this direction for the remainder of the night. Because the southerly wind continued to blow the urban plumes to the site as a cold front passed by, HONO mixing ratios continuously increased to a maximum level of 160 pptv. A slight rainfall started at around 03:00 (PST) on 10 October when HONO mixing ratio started to drop dramatically (Fig. 4).

During this study, HONO and NO_2 generally correlated well as expected (Figs. 4 and 5), indicating that NO_2 might be a key HONO precursor in this environment. Simultaneously there were a few periods when HONO and NO_2 did not correlate well. For instance, on both 3 and 4 October, measured NO_2 mixing ratios were up to 3 ppbv in the late afternoon and early evening because the wind continuously blew from south and southwest without a regular wind shift (Fig. 3). However, when NO_2 reached its peak values, HONO mixing ratios on both days remained at relatively low levels (near or below 50 pptv), possibly because of not enough interaction time between NO_2 and surfaces before the air masses reached the site. The observed HONO-to-NO_2 ratios show a large variability ranging from near 0 to 0.5 (Fig. 4). For a 24-h period, the HONO/NO_2 ratios ranged from 0.05 to 0.13, with a mean ratio of 0.07 (Fig. 5), which is comparable to the ratios at some forested sites in Europe (e.g., Acker et al., 2006b, 2007), but lower than the ratios observed at another forested site at Whiteface Mt., New York (Ren et al., 2006; Zhou et al., 2007), where the average HONO/NO_2 ratios ranged from 0.15 to 0.40.

ACPD
10, 7383–7419, 2010

3.2 Diurnal trends of measured HONO

The diurnal profile during this study shows that the minimum HONO mixing ratios were about ~20–30 pptv in the midday and maximum levels of 60–70 pptv at night (Fig. 5). These daytime HONO levels are lower than levels observed in some other forested sites. For example, at two forested sites in Eastern US (in Whiteface Mountain, New York; Ren et al., 2006) and Europe (in Hohenpeissenberg, Germany; Acker et al., 2006b), daytime HONO levels of 80 to 120 pptv while minima of 20–60 pptv at night were observed. Thus the diurnal pattern of HONO observed at Blodgett Forest is quite different from what was observed in the other two studies. The reasons for these differences are uncertain, but they may be related to the dry climatology and unique diurnal wind pattern (i.e., southwesterly wind during the day and northeasterly wind at night) at Blodgett Forest. Another possible explanation may be related to the acid precipitation in Eastern US and Europe, where soil acidification has occurred (Menz and Seip, 2004). Soil acidification is less prominent in Western US (where Blodgett Forest is located) than in Northeast US and Europe (Fenn et al., 2006), so the heterogeneously formed HONO on the ground surface at Blodgett Forest may be less likely to be released into the atmosphere than at other forest sites where soil acidification is significant. One piece of evidence supporting this hypothesis is the aerosol measurements by an aerosol mass spectrometer (AMS), which confirm that aerosols at Blodgett Forest were close to neutralized (D. Farmer, unpublished data).

The lower soil acidification in Western US than in Eastern US is consistent with the acid precipitation observations by US National Acid Deposition Program (NADP) (http://nadp.sws.uiuc.edu/maps/; select the network (e.g., NTN), map type (e.g., Concentration), analyte (e.g., Filed pH), and year): lower sulfate (SO_4^{2-}) and nitrate (NO_3^-) but higher pH values in the precipitation in Western US than in Eastern US. The precipitation pH in the region of California is basically controlled by the CO_2 equilibrium (pH~5.6) with the influence of high NH_3 emissions from farming activities there. Under less acidic conditions, nitrate photolysis may not be a significant HONO source, and heterogeneous hydrolysis of NO_x may act as a major HONO source. This can explain the different HONO behaviors at Blodgett Forest and at the sites in Eastern US and Europe, i.e., the lower daytime HONO at Blodgett Forest while daytime HONO maxima in Eastern US and Europe (Ren et al., 2006; Acker et al., 2006, 2007) and good correlation between HONO and NO_2 at Blodgett Forest while low correlation (r^2 ~0.01–0.05) in Pinnacle and Whiteface Mountain, New York (Zhou et al., 2002a, 2007).

More evidence supporting this hypothesis came from recent studies in the Artic and Antarctic. In the Arctic significant HONO emissions have been observed from the sunlight-exposed snowpack via the photolysis of HNO_3 and nitrate that originate primarily from the deposition of acidic aerosols transported from North America, Asia and Europe (Zhou et al., 2001; Honrath et al., 2002). In contrast, little HONO was produced from coastal snowpack in the Antarctic where significant sea-salt deposition occurred and NO_3^- ion was present primarily as $NaNO_3$in aged snows, thus preventing the release of or providing a reactive medium for newly formed HONO (Beine et al., 2006). Recent laboratory studies (H. Gao, unpublished data) also found that HONO production from surface HNO_3/nitrate photolysis diminished with higher pH. The rate of HONO production decreased to half for surface NH_4NO_3 photolysis compared to HNO_3 photolysis, but little HONO was produced from surface $NaNO_3$ photolysis, consistent with the results by Beine et al. (2006). While it seems likely to us that the different behaviors of HONO observed at Blodgett Forest are associated with the low soil acidification and acid precipitation in Western US, further studies of HONO in this kind of environment are needed to test this hypothesis.

Temperature dependence of HONO mixing ratios was observed during BEARPEX2007. Figure 6 shows both HONO measurements made by CIMS and LOPAP together with ambient temperature. There were two distinguishing periods: a warm period between 18 August and 12 September, and a cool period from 13 September to 10 October. There was a three-day overlap between CIMS and LOPAP measurements, which will be discussed in detail in Sect. 3.3. Interestingly, the temperature dependence occurred mainly at night, with higher nighttime HONO mixing ratios during the warm period (Fig. 6). During the day, the two periods had very similar observed HONO levels at ~20–40 pptv. This positive temperature dependence of HONO formation has been observed in a chamber study (Rohrer et al., 2005). It is noted that diurnal variations of NO_2 mixing ratios during these two periods are about the same, but the water mixing ratios in the air during the warm period was higher than in the cold period by a factor of 1.2, which may be partially responsible for the difference in the nighttime HONO mixing ratios during these two periods.

During the daytime (08:00–16:00 (PST)), the photolytic loss of HONO is very efficient due to its large photolysis rate coefficients ranging from 0.001 to 0.002 s^{-1}. It is reasonable to assume that HONO reaches photo-steady state (PSS) in the midday. If we assume that only gas phase HONO sources (mainly the OH+NO reaction) are involved in the HONO production, we can then calculate PSS HONO mixing ratios, shown in Fig. 6. The PSS HONO mixing ratios calculated with gas phase HONO sources only are lower than the measurements by a factor of 9 on average, indicating that other HONO sources are dominant in this environment. This result is consistent with previous studies (e.g., Zhou et al., 2002; Acker et al., 2006b, 2007). Calculations also show that a significant HONO source (~1.59 ppbv day^{-1}) is needed in order to sustain the observed HONO level, which presumably comes from heterogeneous processes.

3.3 Intercomparison of LOPAP and CIMS

Time series of HONO measurements collected between 25 and 27 September 2007 by LOPAP and CIMS show very good agreement (Fig. 7), although the CIMS HONO measurements are a little noisy especially at low HONO levels, primarily due to the large uncertainty of the CIMS measurements and a small fraction (~3%) of the CIMS measurement time dedicated to HONO measurement for the need of measuring other species. Using 10-min averages, the linear regression of the CIMS HONO versus the LOPAP HONO produces a slope of 0.94 and an intercept of 4.6 pptv with r^2 of 0.64 (Fig. 7). The fact that LOPAP and CIMS are different techniques for HONO measurements indicates reliable HONO measurements by both instruments, unless both

ACPD
10, 7383–7419, 2010

instruments have the same biases in the HONO measurements. In a recent HONO intercomparison (HINT2009) study in Houston, TX where we deployed our LOPAP instrument, very good agreement was also obtained between LOPAP and four different techniques, including LP-DOAS and tunable infrared laser differential absorption spectrometry (Thomas, 2010).

3.4 NO_y speciation

The sum of reactive nitrogen species in the atmosphere is called NO_y, which is defined here as the sum of NO + NO_2 + HONO + HNO_3 + alkyl nitrates (ANs) + peroxy nitrates (PNs) + HO_2NO_2 + NO_3 + 2×N_2O_5. Box model results show that N_2O_5 and NO_3 were lower than 1 pptv while HO_2NO_2 was typically less than 10 pptv during BEARPEX2007 and thus they do not contribute significantly to the NO_y budget. In the following discussion, we assume that NO_y comprises NO, NO_2, HONO, HNO_3, ANs, and PNs.

Diurnal profiles of reactive nitrogen species exhibit a minimum at 06:00 (PST) and a maximum NO_y at 18:00 (PST) (Fig. 8), due to the primary influence of the Sacramento urban plume and the unique diurnal wind pattern at Blodgett Forest. Similar diurnal variations have been observed in previous studies at this site (e.g., Murphy et al., 2006; Farmer et al., 2008; Day et al., 2009). Among the reactive nitrogen species, NO_2, HNO_3, and PNs are dominant and account for 85% of total NO_y on a 24-h basis (Fig. 8). HONO accounted for only 2.8% of total NO_y on average, with a percentage of 2.2% during the day and 3.3% at night. However, due to fast HONO loss through photolysis, a strong HONO production rate (1.59 ppbv day^{-1}) existed in this environment, suggesting that HONO plays an important role in NO_y cycling. In contrast, HNO_3 production rate from the OH + NO_2 reaction was 0.53 ppbv day^{-1} on average, which is only one third of the HONO production rate.

The production of NO from the photolysis of HONO may potentially affect the cycling between NO_2 and NO. Calculations show that the HONO photolysis rate was only about 1.5% of the NO_2 photolysis rate, indicating that that HONO photolysis did not significantly influence the NO-NO_2 cycling, mainly due to the low HONO levels during the day and fast cycling between NO_2 and NO.

3.5 Contribution of HONO photolysis to HO_x production

A box model based on the Regional Atmospheric Chemistry Mechanism (RACM) (Stockwell et al., 1997) was developed to interpret the field measurements and investigate atmospheric oxidation chemistry in this environment. The model was constrained by the available simultaneous measurements in this study and calculated concentrations of free radicals, such as OH, HO_2, and RO_2. Similar model simulations have been conducted in previous studies (e.g., Ren et al., 2003, 2006). Using the model results, the contribution of HONO photolysis to HO_x production can be calculated.

The diurnal profile of HO_x production shows that HO_x production was primarily from the photolysis of HCHO and O_3 during the day, while nighttime HO_x was mainly produced from O_3 + alkene reactions (Fig. 9). The photolysis of HONO did not contribute significantly to HO_x production even in the early morning due to its relatively low mixing ratios. On a 24-h basis, HONO photolysis only accounted for about 6% of total HO_x production.

The insignificant contribution of HONO photolysis to HO_x production at Blodgett Forest is in contrast with the results from some studies at other forested sites. For instance, at a forested site in Whiteface Mountain, Northern New York State, HONO photolysis was found to be a dominant HO_x source in the early morning and late afternoon with an overall contribution of 34% to HO_x production on a 24-h basis (Ren et al., 2006). At another rural site in New York State, the average radical production from HONO photolysis was 2.3 ppbv day^{-1} and accounted for 24% of the total HO_x production (Zhou et al., 2002a). In a study at the Meteorological Observatory Hohenpeissenberg in Germany, HONO photolysis was also found to be a dominant HO_x source in the early morning and the overall contribution of HONO photolysis comprised 42% of total photolytic HO_x production (Acker et al., 2006a). Klaffmannn et al. (2005) found that HONO photolysis contributed about 33% of total OH production in a forest in Jülich, Germany.

The reasons for the smaller HONO mixing ratios and thus smaller contribution of HONO photolysis to HO_x production at Blodgett Forest are uncertain. As discussed previously, it may be related to the dry climatology and low acid precipitation in this water-limited environment.

4 Conclusions

The measurement suite of HONO and other NO_y species during BEARPEX2007 at Blodgett Forest in summer/fall 2007 provides a great opportunity to study nitrogen chemistry in this forested environment. Measured HONO mixing ratios show a diurnal pattern with minimum levels of ~20–30 pptv during the day and maximum levels of ~60–70 pptv at night, which is significantly different from the results at other forested sites in Eastern US and Europe. The daytime HONO levels at Blodgett Forest are significantly lower compared to the other forested sites where minimum HONO levels during the day and maximum levels at night were often observed. This different diurnal pattern may be related to the unique diurnal wind pattern (i.e., upslope wind during the day and downslope wind at night), dry climatology, and low acid precipitation at Blodgett Forest. Intercomparison of HONO measurements by two different techniques, LOPAP and CIMS, shows very good agreement, indicating reliable HONO measurements by both instruments. Although HONO only accounted for only 3% of total NO_y on average, a strong HONO production rate (1.59 ppbv day^{-1}) existed in this environment, indicating a fast cycling from other forms of NO_y to HONO.

Because of relatively low mixing ratios of HONO in this environment, the photolysis of HONO did not contribute significantly to HO_x production during this study. This is quite different from some studies in other forested areas, where HONO photolysis was typically found to be a dominant or at least an important HO_x source. Further studies on HONO seasonal variations and HONO vertical fluxes are needed in order to improve our understanding of atmospheric oxidation and nitrogen budget in this kind of water-limited and anthropogenic pollution influenced environment with high biogenic emissions.

ACPD
10, 7383–7419, 2010

Acknowledgements. The authors would like to thank Sierra Pacific Industries for the use of their land and the University of California, Berkeley, Center for Forestry, Blodgett Forest Research Station for cooperation in facilitating this study. The authors also thank other research groups participating in this field study for the use of their data in the analysis. This study was partially supported by a National Science Foundation grant (ATM-0914619).

References

Acker, K., Febo, A., Trick, S., Perrino, C., Bruno, P., Wiesen, P., Möller, D., Wieprecht, W., Auel, R., Giusto, M., Geyer, A., Platt, U., and Allegrini, I.: Nitrous acid in the urban area of Rome, Atmos. Environ., 40, 3123–3133, 2006a.

Acker, K., Möller, D., Wieprecht, W., Meixner, F. X., Bohn, B., Gilge, S., Plass-Dülmer, C., and Berresheim, H.: Strong production of OH from HNO_2 at a rural mountain site, Geophys. Res. Lett., 33, L02809, doi:10.1029/2005GL024643, 2006b.

Acker, K. and Möller, D.: Atmospheric variation of nitrous acid at different sites in Europe, Environ. Chem., 4, 242–255, 2007.

Alicke, B., Geyer, A., Hofzumahaus, A., Holland, F., Konrad, S., Pätz, H. W., Schäfer, J., Stutz, J., Volz-Thomas, A., and Platt, U.: OH formation by HONO photolysis during the BERLIOZ experiment, J. Geophys. Res., 108, 8247, doi:10.1029/2001JD000579, 2003.

Allegrini, I., Cortiello, M., Febo, A., and Perrino, C.: Generation of standard atmospheres of nitrous acid, In Physico-Chemical Behaviour of Atmospheric Pollutants, Kluwer Academic Publishers, Dodrecht, 140–144, 1990.

Ammann, M., Kalberer, M., Jost, D. T., Tobler, L., Rössler, E., Piguet, D., Gäggeler, H. W., and Baltensperger, U.: Heterogeneous production of nitrous acid on soot in polluted air masses, Nature, 395, 157–160, 1998.

Appel, B. R., Winer, A. M., Tokiwa, Y., and Biermann, H. W.: Comparison of atmospheric nitrous acid measurements by annular denuder and optical absorption systems, Atmos. Environ., 24A, 611–616, 1990.

Arens, F., Gutzwiller, L., Baltensperger, U., Gäggeler, H. W., and Ammann, M.: Heterogeneous reaction of NO_2 on diesel soot particles, Environ. Sci. Technol., 35, 2191–2199, 2001.

Aubin, D. G. and Abbatt, J. P. D.: Interaction of NO_2 with hydrocarbon soot: Focus on HONO yield, surface modification, and mechanism, J. Phys. Chem. A, 111, 6263–6273, 2007.

Beine, H. J., Amoroso, A., Domin, F., King, M. D., Nardino, M., Ianniello, A., and France, J. L.: Surprisingly small HONO emissions from snow surfaces at Browning Pass, Antarctica, Atmos. Chem. Phys., 6, 2569–2580, 2006, http://www.atmos-chem-phys.net/6/2569/2006/.

Bejan, I., Abd-el-Aal, Y., Barnes, I., Benter, T., Bohn, B., Wiesen, P., and Kleffmann, J.: The photolysis of ortho-nitrophenols: a new gas phase source of HONO, Phys. Chem. Chem. Phys., 8, 2028–2035, 2006.

Bouvier-Brown, N. C., Goldstein, A. H., Gilman, J. B., Kuster, W. C., and de Gouw, J. A.: In-situ ambient quantification of monoterpenes, sesquiterpenes, and related oxygenated compounds during BEARPEX 2007: implications for gas- and particle-phase chemistry, Atmos. Chem. Phys., 9, 5505–5518, 2009, http://www.atmos-chem-phys.net/9/5505/2009/.

Bröske, R., Kleffmann, J., and Wiesen, P.: Heterogeneous conversion of NO_2 on secondary organic aerosol surfaces: A possible source of nitrous acid (HONO) in the atmosphere?, Atmos. Chem. Phys., 3, 469–474, 2003, http://www.atmos-chem-phys.net/3/469/2003/.

Carr, S., Heard, D. E., and Blitz, M. A.: Comment on “Atmospheric hydroxyl radical production from electronically excited NO_2 and H_2O”, Science, 324, 336b, doi:10.1126/science.1166669, 2009.

Crounse, J. D., McKinney, K. A., Kwan, A. J., and Wennberg, P. O.: Measurement of gas-phase hydroperoxides by chemical ionization mass spectrometry, Anal. Chem., 78, 6726–6732, 2006.

Day, D. A., Farmer, D. K., Goldstein, A. H., Wooldridge, P. J., Minejima, C., and Cohen, R. C.: Observations of NO_x, $\sum$PNs, $\sum$ANs, and HNO_3 at a Rural Site in the California Sierra Nevada Mountains: summertime diurnal cycles, Atmos. Chem. Phys., 9, 4879–4896, 2009, http://www.atmos-chem-phys.net/9/4879/2009/.

Elshorbany, Y. F., Kurtenbach, R., Wiesen, P., Lissi, E., Rubio, M., Villena, G., Gramsch, E., Rickard, A. R., Pilling, M. J., and Kleffmann, J.: Oxidation capacity of the city air of Santiago, Chile, Atmos. Chem. Phys., 9, 2257–2273, 2009, http://www.atmos-chem-phys.net/9/2257/2009/.

Faloona, I. C., Tan, D., Lesher, R. L., Hazen, N. L., Frame, C. L., Simpas, J. B., Harder, H., Martinez, M., Di Carlo, P., Ren, X., and Brune, W. H.: A laser-induced fluorescence instrument for detecting tropospheric OH and HO_2: Characteristics and calibration, J. Atmos. Chem.,

47, 139–167, 2004.
Farmer, D. K. and Cohen, R. C.: Observations of HNO_3, $\sum$AN, $\sum$PN and NO_2 fluxes: evidence for rapid HOx chemistry within a pine forest canopy, Atmos. Chem. Phys., 8, 3899–3917, 2008, http://www.atmos-chem-phys.net/8/3899/2008/.
Febo, A., Perrino, C., Gherardi, M., and Sparapani, R.: Evaluation of a high-purity and high-stability continuous generation system for nitrous acid, Environ. Sci. Technol., 29, 2390–2395, 1995.
Febo, A., Perrino, C., and Allegrini, I.: Measurement of nitrous acid in Milan, Italy, by DOAS and diffusion denuders, Atmos. Environ., 30, 3599–3609, 1996.
Fenn, M. E., Huntington, T. G., McLaughlin, S. B., Eagar, C., Gomez, A., and Cook, R. B.: Status of soil acidification of North America, J. Forest Sci., 52, 3–13, 2006.
Finlayson-Pitts, B. J., Wingen, L. M., Sumner, A. L., Syomin, D., and Ramazan, K. A.: The heterogeneous hydrolysis of NO_2 in laboratory systems and in outdoor and indoor atmospheres: An integrated mechanism, Phys. Chem. Chem. Phys., 5, 223–242, 2003.
George, C., Strekowski, R. S., Kleffmann, J., Stemmler, K., and Ammann, M.: Photoenhanced uptake of gaseous NO_2 on solid organic compounds: A photochemical source of HONO, Faraday Discussion, 130, 195–210, 2005.
Goldstein, A. H., Hultman, N. E., Fracheboud, J. M., Bauer, M. R., Panek, J. A., Xu, M., Qi, Y., Guenther, A. B., and Baugh, W.: Effects of climate variability on the carbon dioxide, water, and sensible heat fluxes above a ponderosa pine plantation in the Sierra Nevada (CA), Agr. Forest Meteorol., 101, 113–129, 2000.
Harrison, R. M., Peak, J. D., and Collins, G. M.: Tropospheric cycle of nitrous acid, J. Geophys. Res., 101, 14429–14439, 1996.
Heland, J., Kleffmann, J., Kurtenbach, R., and Wiesen, P.: A new instrument to measure gaseous nitrous acid (HONO) in the atmosphere, Environ. Sci. Technol., 35, 3207–3212, 2001.
Hirokawa, J., Kato, T., and Mafuné, F.: In situ measurements of atmospheric nitrous acid by chemical ionization mass spectrometry using chloride ion transfer reactions, Anal. Chem., 81, 8380–8386, 2009.
Honrath, R. E., Lu, Y., Peterson, M. C., Dibb, J. E., Arsenault, M. A., Cullen, N. J., and Steffen, K.: Vertical fluxes of NO_x, HONO, and HNO_3 above the snowpack at Summit, Greenland, Atmos. Environ., 36, 2629–2640, 2002.

Huang, G., Zhou, X., Deng, G., Qiao, H., and Civerolo, K.: Measurements of atmospheric nitrous acid and nitric acid, Atmos. Environ., 36, 2225–2235, 2002.
Kleffmann, J., Heland, J., Kurtenbach, R., Lörzer, J. C., and Wiesen, P.: A new instrument (LOPAP) for the detection of nitrous acid (HONO), Environ. Sci. Pollut. Res., 9, 48–54, 2002.
Kleffmann, J., Kurtenbach, R., Lörzer, J. C., Wiesen, P., Kalthoff, N., Vogel, B., and Vogel, H.: Measured and simulated vertical profiles of nitrous acid. Part I: Field measurements, Atmos. Environ., 37, 2949–2955, 2003.
Kleffmann, J., Gavriloaiei, T., Hofzumahaus, A., Holland F., Koppmann, R., Rupp, L., Schlosser, E., Siese, M., and Wahner, A.: Daytime formation of nitrous acid: a major source of OH radicals in a forest, Geophys. Res. Lett., 32, L05818, doi:10.1029/2005GL022524, 2005.
Kleffmann, J., Lörzer, J. C., Weisen, P., Kern, C., Trick, S., Volamer, R., Rodenas, M., and Wirtz, K.: Intercomparison of the DOAS and LOPAP techniques for the detection of nitrous acid (HONO), Atmos. Environ., 40, 3640–3652, 2006.
Kleffmann, J. and Wiesen, P.: Technical Note: Quantification of interferences of wet chemical HONO LOPAP measurements under simulated polar conditions, Atmos. Chem. Phys., 8, 6813–6822, 2008, http://www.atmos-chem-phys.net/8/6813/2008/.
LaFranchi, B. W., Wolfe, G. M., Thornton, J. A., Harrold, S. A., Browne, E. C., Min, K. E., Wooldridge, P. J., Gilman, J. B., Kuster, W. C., Goldan, P. D., de Gouw, J. A., McKay, M., Goldstein, A. H., Ren, X., Mao, J., and Cohen, R. C.: Closing the peroxy acetyl nitrate budget: observations of acyl peroxy nitrates (PAN, PPN, and MPAN) during BEARPEX 2007, Atmos. Chem. Phys., 9, 7623–7641, 2009, http://www.atmos-chem-phys.net/9/7623/2009/.
Langridge, J. M., Gustafsson, R. J., Griffiths, P. T., Cox, R. A., Lambert, R. M., and Jones, R. L.: Solar driven nitrous acid formation on building material surfaces containing titanium dioxide: A concern for air quality in urban areas?, Atmos. Environ., 43, 5128–5131, 2009.
Li, S., Mathews, J., and Sinha, A.: Atmospheric hydroxyl radical production from electronically excited NO_2 and H_2O, Science, 319, 1657–1660, 2008.
Mao, J., Ren, X., Chen, S., Brune, W. H., Chen, Z., Martinez, M., Harder, H., Lefer, B., Rappenglück, B., Flynn, J., and Leuchner, M.: Atmospheric oxidation capacity in the summer of Houston 2006: Comparison with summer measurements in other metropolitan studies, Atmos. Environ., 44, doi:10.1016/j.atmosenv.2009.01.013, in press, 2010.
Menz, F. C. and Seip, H. M.: Acid rain in Europe and the United States: an update, Environ.

Sci. Policy, 7, 253–265, 2004.
Murphy, J. G., Day, D. A., Cleary, P. A., Wooldridge, P. J., and Cohen, R. C.: Observations of the diurnal and seasonal trends in nitrogen oxides in the western Sierra Nevada, Atmos. Chem. Phys., 6, 5321–5338, 2006, http://www.atmos-chem-phys.net/6/5321/2006/.
Neftel, A., Blatter, A., Hesterberg, R., and Staffelbach, T.: Measurements of concentration gradients of HNO_2 and HNO_3 over a semi-natural ecosystem, Atmos. Environ., 30, 3017–3025, 1996.
Park, J.-Y. and Lee, Y.-N.: Solubility and decomposition kinetics of nitrous acid in aqueous solution, J. Phys. Chem., 92, 6294–6302, 1988.
Pérez, I. M., Wooldridge, P. J., and Cohen, R. C.: Laboratory evaluation of a novel thermal dissociation chemiluminescence method for in situ detection of nitrous acid, Atmos. Environ., 41, 3993–4001, 2007.
Qin, M., Xie, P., Su, H., Gu, J., Peng, F., Li, S., Zeng, L., Liu, J., Liu, W., and Zhang, Y.: An observational study of the HONO-NO_2 coupling at an urban site in Guangzhou City, South China, Atmos. Environ., 43, 5731–5742, doi:10.1016/j.atmosenv.2009.08.017, 2009.
Ren, X., Harder, H., Martinez, M., Lesher, R. L., Oliger, A., Simpas, J. B., Brune, W. H., Schwab, J. J., Demerjian, K. L., He, Y., Zhou, X., and Gao, H.: OH and HO_2 chemistry in the urban atmosphere of New York City, Atmos. Environ., 37, 3639–3651, 2003.
Ren, X., Brune, W. H., Oliger, A., Metcalf, A. R., Simpas, J. B., Shirley, T., Schwab, J. J., Bai, C., Roychowdhury, U., Li, Y., Cai, C., Demerjian, K. L., He, Y., Zhou, X., Gao, H., and Hou, J.: OH, HO_2 and OH Reactivity during the PMTACS–NY Whiteface Mountain 2002 Campaign: Observations and Model Comparison, J. Geophys. Res., 111, D10S03, doi:10.1029/2005JD006126, 2006.
Schartz, S. E. and White, W. H.: Solubility equilibria of the nitrogen oxides and oxyacids in dilute aqueous solution, Adv. Environ. Sci. Eng., 1–45, 1981.
Staffelbach, T., Neftel, A., and Horowitz, L. W.: Photochemical oxidant formation over southern Switzerland 2. Model results, J. Geophys. Res., 102, 23363–23373, 1997.
Stemmler, K., Ammann, M., Dondors, C., Kleffmann, J., and George, C.: Photosensitized reduction of nitrogen dioxide on humic acid as a source of nitrous acid, Nature, 440, 195–198, 2006.
Stockwell, W. R., Kirchner, F., and Kuhn, M.: A new mechanism for regional atmospheric chemistry modeling, J. Geophys. Res., 102, 25847–25879, 1997.

Stutz, J., Oha, H.-J., Whitlow, S. I., Anderson, C., Dibb, J. E., Flynn, J. H., Rappenglück, B., and Lefer, B.: Simultaneous DOAS and mist-chamber IC measurements of HONO in Houston, TX, Atmos. Environ., 44, doi:10.1016/j.atmosenv.2009.02.003, in press, 2010.

Thornton, J. A., Wooldridge, P. J., and Cohen, R. C.: Atmospheric NO_2: In situ laser-induced fluorescence detection at parts per trillion mixing ratios, Anal. Chem., 72, 528–539, 2000.

Vogel, B., Vogel, H., Kleffmann, J., and Kurtenbach, R.: Measured and simulated vertical profiles of nitrous acid, Part II – model simulations and indications for a photolytic source, Atmos. Environ., 37, 2957–2966, 2003.

Winer, A. M., and Biermann, H. W.: Long pathlength differential optical absorption spectroscopy (DOAS) measurements of gaseous HONO, NO_2 and HCHO in the California South Coast Air Basin, Res. Chem. Intermed., 20, 423–445, 1994.

Wolfe, G. M., Thornton, J. A., Yatavelli, R. L. N., McKay, M., Goldstein, A. H., LaFranchi, B., Min, K.-E., and Cohen, R. C.: Eddy covariance fluxes of acyl peroxy nitrates (PAN, PPN and MPAN) above a Ponderosa pine forest, Atmos. Chem. Phys., 9, 615–634, 2009, http://www.atmos-chem-phys.net/9/615/2009/.

Yokelson, R. J., Crounse, J. D., DeCarlo, P. F., Karl, T., Urbanski, S., Atlas, E., Campos, T., Shinozuka, Y., Kapustin, V., Clarke, A. D., Weinheimer, A., Knapp, D. J., Montzka, D. D., Holloway, J., Weibring, P., Flocke, F., Zheng, W., Toohey, D., Wennberg, P. O., Wiedinmyer, C., Mauldin, L., Fried, A., Richter, D., Walega, J., Jimenez, J. L., Adachi, K., Buseck, P. R., Hall, S. R., and Shetter, R.: Emissions from biomass burning in the Yucatan, Atmos. Chem. Phys., 9, 5785–5812, 2009, http://www.atmos-chem-phys.net/9/5785/2009/.

Zhou, X., Beine, H. J., Honrath, R. E., Fuentes, J. D., Simpson, W., Shepson, P. B., and Bottenheim, J. W.: Snowpack photochemical production of HONO: A major source OH in the Arctic boundary layer in springtime, Geophys. Res. Lett., 28, 4087–4090, 2001.

Zhou, X., Civerolo, K., Dai, H., Huang, G., Schwab, J., and Demerjian, K.: Summertime nitrous acid chemistry in the atmospheric boundary layer at a rural site in New York State, J. Geophys. Res., 107, 4590, doi:10.1029/2001JD001539, 2002a.

Zhou, X., He, Y., Huang, G., Thornberry, T. D., Carroll, M. A., and Bertman, S. B.: Photochemical production of nitrous acid on glass sample manifold surface, Geophys. Res. Lett., 29, 1681, doi:10.1029/2002GL015080, 2002b.

Zhou, X., Gao, H., He, Y., Huang, G., Bertman, S., Civerolo, K., and Schwab, J.: Nitric acid photolysis on surfaces in low-NO_x environments: significant atmospheric implications, Geophys.

Res. Lett., 30, 2217, doi:10.1029/2003GL018620, 2003.
Zhou, X., Huang, G., Civerolo, K., Roychowdhury, U., and Demerjian, K. L.: Summertime observations of HONO, HCHO, and O_3 at the summit of Whiteface Mountain, New York, J. Geophys. Res., 112, D08311, doi:10.1029/2006JD007256, 2007.
Ziemba, L. D., Dibb, J. E., Griffin, R. J., Anderson, C. H., Whitlow, S. I., Lefer, B. L., Rappenglück, B., and Flynn, J.: Heterogeneous conversion of nitric acid to nitrous acid on the surface of primary organic aerosol in an urban atmosphere, Atmos. Environ., 44, doi:10.1016/j.atmosenv.2008.12.024, in press, 2010.

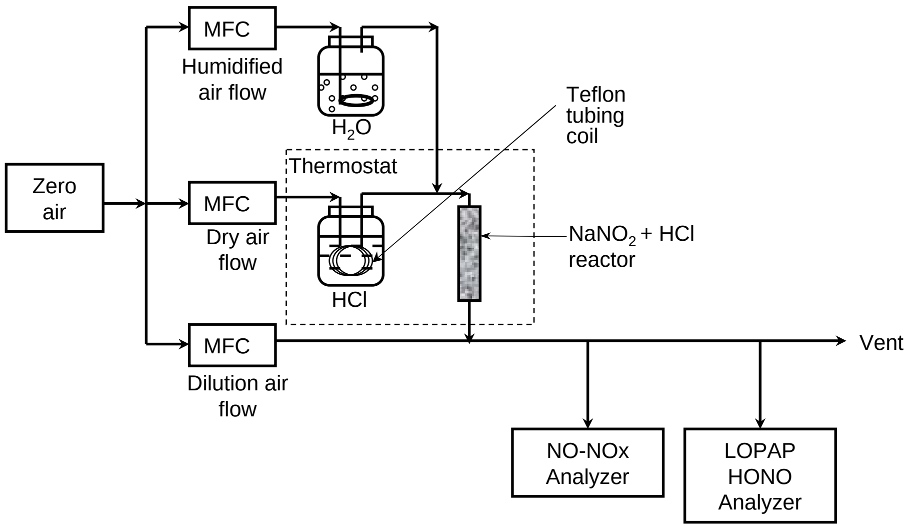

Fig. 1. Schematic of a HONO generation system. MFC represents a mass flow controller.

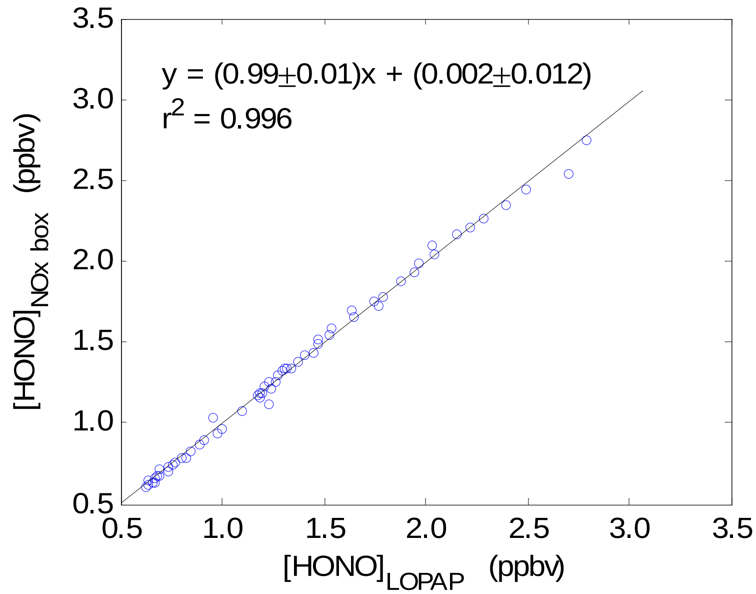

Fig. 2. Comparison of HONO measurements with a LOPAP-HONO instrument and a TEI NO-NO_x analyzer when both instruments sampled a HONO source. The HONO source was produced by a HONO generation system.

ACPD
10, 7383–7419, 2010

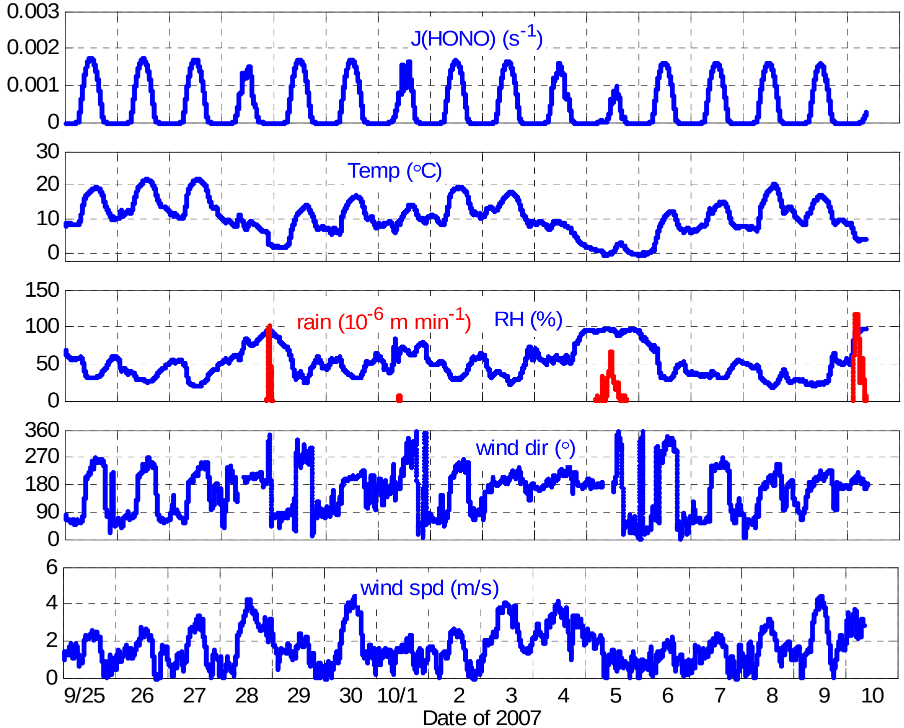

Fig. 3. Time series of HONO photolysis frequency, ambient temperature, relative humidity, rain fall, wind direction, and wind speed between 25 September and 10 October 2007 during BEARPEX2007 when the LOPAP HONO measurements were available.

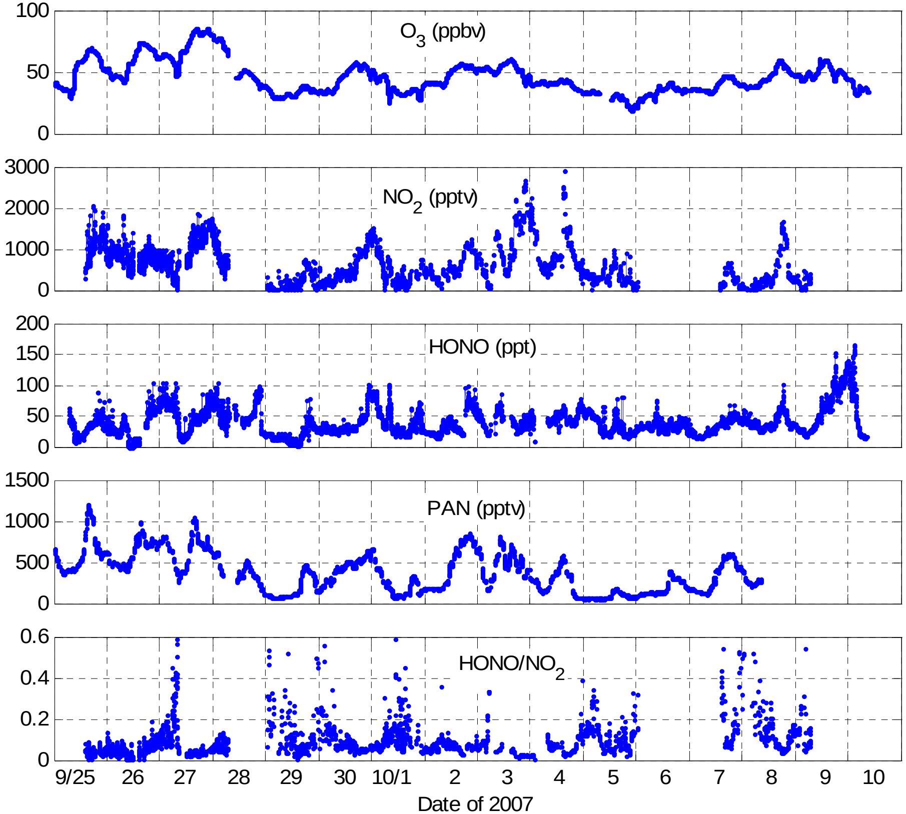

Fig. 4. Time series of measured ozone, NO_2, PAN, HONO, and HONO/NO_2 ratio between 25 September and 10 October during BEARPEX2007. HONO measurements made by LOPAP are shown.

ACPD
10, 7383–7419, 2010

Atmospheric nitrous acid at Blodgett Forest

X. Ren et al.

ACPD

10, 7383–7419, 2010

Atmospheric nitrous acid at Blodgett Forest

X. Ren et al.

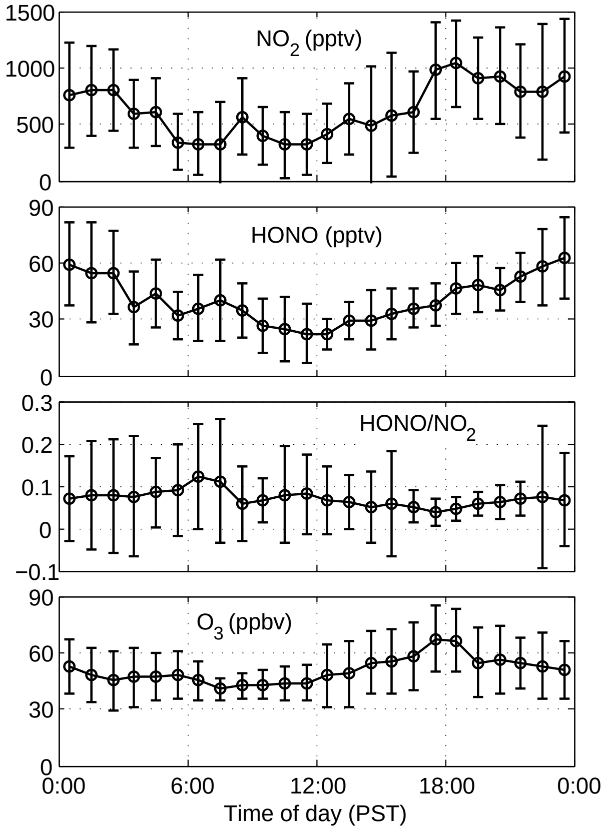

Fig. 5. Average diurnal profiles of O_3, NO_2, HONO, and HONO/NO_2. HONO was measured at a height of 14 m (~6 m above the canopy) by the LOPAP instrument and NO_2 was measured at a height of 12.7 m. The data were collected between 25 September and 10 October during BEARPEX2007. Error bars represent standard deviations in hourly bins.

ACPD

10, 7383–7419, 2010

Atmospheric nitrous acid at Blodgett Forest

X. Ren et al.

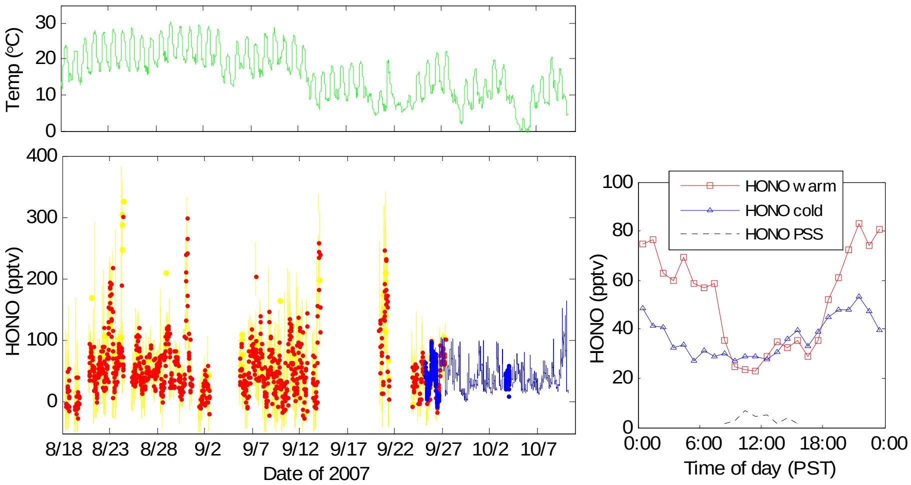

Fig. 6. Left: time series of ambient temperature (in green) and measured HONO mixing ratios by CIMS (1 min averages in yellow and 10 min averages in red) and by LOPAP (in blue). Right: diurnal variations of HONO mixing ratios during the warm period (red squares) and cool period (blue triangles). Also plotted are the photo-steady state (PSS) HONO mixing ratios (dashed black line) averaged for the entire study. In the PSS calculation, only gas phase HONO sources are included during the day between 08:00 and 16:00 (PST).

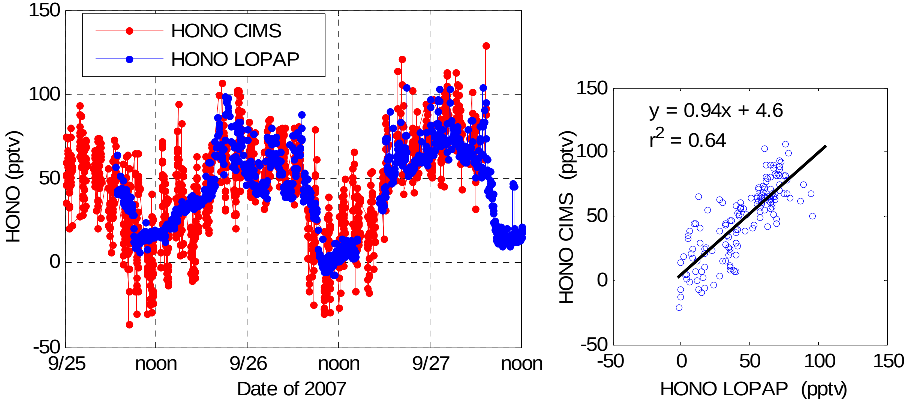

Fig. 7. Comparison of HONO measurements by LOPAP (blue dots) and CIMS (red dots) over three days between 25 and 27 September 2007. Left: time series. Right: scatter plot of CIMS HONO versus LOPAP HONO with 10-min averages.

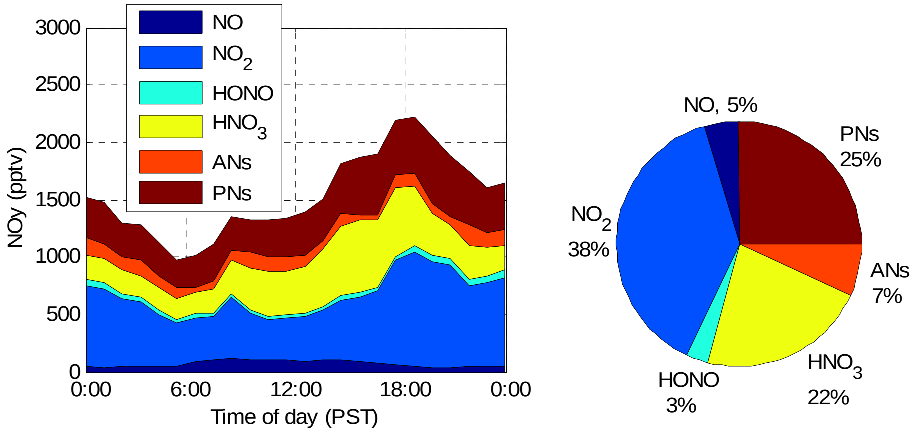

Fig. 8. Median diurnal variations (left) and distribution (right) of NO_y species during BEARPEX2007. ANs represents total alkyl nitrates and PNs represents total peroxy nitrates. The pie chart is representative of a 24-h basis. Data collected between 15 August and 10 October 2007 are used in this figure.

ACPD
10, 7383–7419, 2010

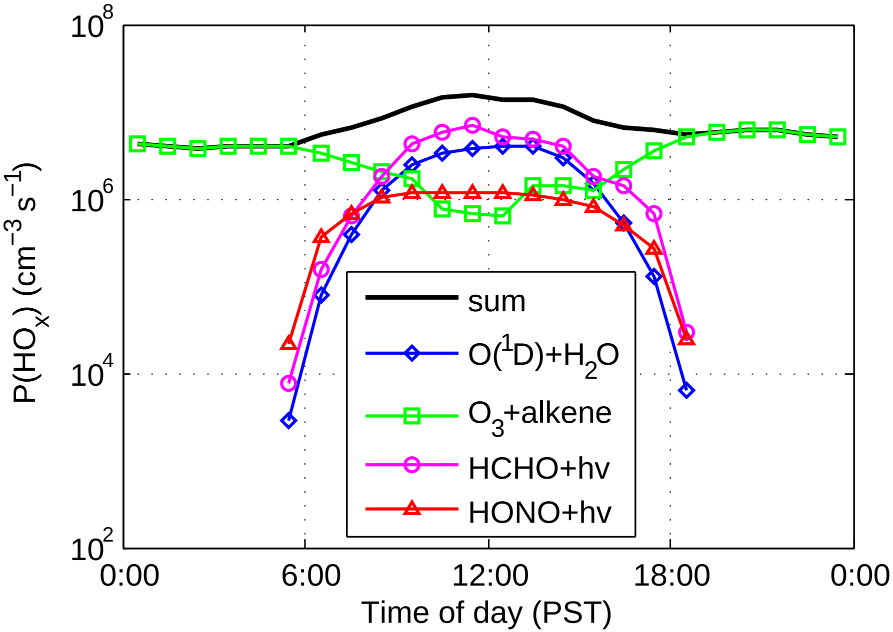

Fig. 9. Diurnal variation of HO_x production rates from the photolysis of ozone followed by the consequent $O(^1D)+H_2O$ reaction (diamonds), the photolysis of HCHO (circles), the photolysis of HONO (triangles), and from the reactions of O_3+alkenes (squares). The total HO_x production rate is shown as a black line.

ACPD
10, 7383–7419, 2010

Atmospheric nitrous acid at Blodgett Forest

X. Ren et al.